Growth of intact water ice on Ru(0001) between 140 and 160 K: Experiment and density-functional theory calculations

S. Haq, C. Clay, G. R. Darling, G. Zimbitas, and A. Hodgson
Surface Science Research Centre, The University of Liverpool, Liverpool L693BX, United Kingdom
(Received 12 December 2005; published 15 March 2006)

We report low-energy electron diffraction (LEED) and reflection absorption IR spectroscopy (RAIRS) results for water adsorption on Ru(0001) at temperatures between 140 and 160 K, where water forms intact hydrogen bonded structures on the surface. We find that H_2O and D_2O adsorption show identical behavior, with no evidence for a structural isotope effect. At low coverage LEED shows a diffuse $(\sqrt{3}\times\sqrt{3})R30°$ pattern, which becomes sharp and intense only as the coverage reaches 0.6 to 0.67 monolayer. The LEED pattern becomes broadened and diffuse as the surface saturates with a coverage of 0.76 monolayer. In RAIRS the low-frequency bands associated with the out of plane libration of hydrogen bonded water appear at low coverage, with the water stretch and scissors bands appearing as broad bands only as the coverage is increased. Water adsorbs flat on Ru(0001) at low coverage, forming small clusters which buckle to create an extended, hydrogen bonded structure only as the adlayer is completed. The free OH(OD) stretch band appears only as the monolayer approaches completion, indicating flat or H-down adsorption up to 0.67 monolayer with H-up water appearing as the $\sqrt{3}$ structure compresses. Density functional calculations at low coverage find that water forms stable clusters with water adsorbed flat on the surface. Calculations for a complete 0.67 monolayer structure find water adsorbed near the Ru atop site in a hydrogen bonded honeycomb network, containing chains of "flat" lying water, linked by upright chains bonded "H down" in the hexagonal, hydrogen bonded superstructure. This structure is ~20% more stable than the conventional ice bilayer structure and is expected to wet the Ru(0001) surface. We propose a model in which disordered, short chains of "flat" and H-down water are imbedded in a honeycomb network of hydrogen bonded water, which imposes long-range order on the adlayer but allows substantial local disorder, and discuss the agreement with existing experimental results.

DOI: 10.1103/PhysRevB.73.115414 PACS number(s): 68.43.Fg, 68.43.Mn, 68.35.−p, 82.30.Rs

I. INTRODUCTION

Understanding water adsorption at metal surfaces is a prerequisite for unravelling the behavior of aqueous metal interfaces, many of which play key roles in technologically important processes, such as in electrochemical fuel cells, catalysis, and corrosion. Despite this, our knowledge of the structure and dynamics of water adsorption remains surprisingly limited, with a number of fundamental questions still to be resolved before general models can be developed for the structure of water at metal surfaces.[1,2] Conventionally, water is thought to form an extended, hydrogen bonded bilayer on close packed metal surfaces, similar to the (0001) planes found in bulk ice Ih. This structure contains hexagonal rings, with three water molecules in each ring bound via O to the surface and another three water molecules above them completing the hydrogen bonded "bilayer" structure.[1] However, recent density functional theory (DFT) calculations suggest that the binding energy of the "bilayer" structure[1] is insufficient for water to wet Ru(0001) (Ref. 3) (or other transition metal surfaces[4]). Instead Feibelman proposed a partially dissociated adlayer,[3] starting a debate about the structure and chemical identity of water on Ru(0001).[3,5–10]

Commensurate $(\sqrt{3}\times\sqrt{3})R30°$ ice structures have been reported on several close packed metal surfaces,[1,2] including Ru(0001).[11,12] Held and Menzel observed a $\sqrt{3}$ structure for D_2O but not for H_2O adsorption,[13] a result which they attributed to a structural isotope effect.[14] Simulation of low-energy electron diffraction intensity measurements (LEED IV) found that the D_2O structure was almost flat, with an O buckling of just 0.07 Å (Ref. 8) compared to 0.96 Å in ice Ih. Again, this is inconsistent with DFT calculations which found a much greater buckling for an intact bilayer structure.[3] In contrast the calculations suggested a partially dissociated structure was more stable, containing hydrogen bonded rings of OD and D_2O with O almost coplanar and D either adsorbed atop bare Ru or as separate islands. A reinvestigation of the LEED IV results still preferred an intact water model—although it could not exclude the partially dissociated structure.[8] Recently we reported reflection absorption IR (RAIRS) and thermal desorption measurements which indicate that water adsorbs intact at low temperatures, dissociation being activated and occurring above 160 K for H_2O to form a stable, planar mixed $H/OH/H_2O$ structure.[10] Dissociation shows a strong isotope effect,[15] with D_2O desorbing intact as the film is heated to 170 K, leaving no O or D on the surface, whereas H_2O undergoes partial desorption ($A2$ feature) but then stabilizes a partially dissociated layer containing 0.46 ML water adsorbed as $H/OH/H_2O$.[10] A partially dissociated overlayer can also be formed by reacting O with either H_2O or D_2O.[10] XPS shows that water adsorbs intact but dissociates rapidly under electron exposure,[16] with both OH and H_2O present in the high temperature ($A1$) phase.[17] These results support Feibelman's suggestion that a partially dissociated overlayer is the stable phase on Ru(0001) (Ref. 3) and imply that the intact water adlayer formed at low temperature is metastable with respect to dissociation.[10] However, these results do not resolve the dis-

crepancy between the different structures found for H_2O and D_2O in LEED,[8] nor explain how intact water wets the surface when DFT calculations find too low a binding energy.[3,4]

We have examined the growth of water adlayers on Ru(0001) with LEED, RAIRS, and temperature programmed desorption (TPD), using DFT calculations to relate our experimental observations to different structural motifs. Water was adsorbed at temperatures between 140 and 155 K, where it is mobile and forms ordered hydrogen bonding structures but does not dissociate to form the mixed $H/OH/H_2O$ structures. Both H_2O and D_2O show identical adsorption behavior, forming $(\sqrt{3}\times\sqrt{3})R30°$ LEED patterns which sharpen only as the coverage approaches 2/3 monolayer and a complete water layer is formed. Changes in the relative intensities of the libration and stretching bands in RAIRS indicate a change from a flat lying to a buckled water geometry as the clusters formed at low coverage are converted into a complete adlayer with water adsorbed "H down." Further uptake occurs before adsorption saturates with a coverage of 0.76 ML and a faint $\sqrt{3}$ LEED pattern. DFT calculations find that flat lying water clusters are formed at low coverage, and are more stable than water adsorbed in the standard buckled $(\sqrt{3}\times\sqrt{3})R30°$-$2H_2O$ bilayer. Growth of these flat water clusters is unfavorable as some water must buckle out of plane, destabilising adsorption. Calculations find that the complete, ordered 2/3 ML structure forms a stable honeycomb hydrogen bonding structure with water arranged in rows of flat and rows of "H-down" water, rather than in the conventional bilayer structure. We discuss this model and argue that an extended honeycomb hydrogen bonding structure in which water is predominantly adsorbed as disordered chains of "flat" and "H-down" water is consistent with the existing data for intact low-temperature water adsorption on Ru(0001).

II. EXPERIMENTAL

Water was dosed onto the Ru(0001) surface for LEED and temperature programmed desorption measurements (TPD) using a collimated, differentially pumped molecular beam which produced a 5 mm adsorption spot on the crystal.[10] This allowed the isotopic purity of the water sample, either triply distilled H_2O or D_2O (99.9% D), to be transferred directly to the surface without contamination by displacement of water adsorbed on the chamber walls. Saturation of the gas line and beam was achieved by running several changes of the required isotope through the beam line prior to the experiment. This is particularly important for D_2O which adsorbs and desorbs intact only when isotopicly pure. Desorption was monitored by a QMS placed in direct line of sight of the sample. The Ru(0001) crystal was spot welded to Ta heating wires and to liquid nitrogen cooled Ta posts. Temperature was controlled by a computer controlled dc current supply, allowing the surface to be held at a fixed temperature for dosing, ramped ($\leqslant$10 K s^{-1}) for temperature programmed desorption (TPD) or stepped to a new temperature for isothermal desorption measurements. Water was typically dosed at 0.0075 ML s^{-1} and the uptake measured using the direct reflection technique and calibrated against the coverage of water required to saturate the $(\sqrt{39}\times\sqrt{39})R16°$ water layer on Pt(111).[18,19] This was taken to have a density of 1.23×10^{15} cm^{-2} and provides an independent measure of water coverage, avoiding any assumptions about the coverage of water required to form the various LEED patterns seen on Ru(0001). Water coverages are given as monolayers (ML) relative to the surface density of Ru(0001). The overall precision of this uptake calibration relative to the saturated monolayer on Pt(111) is estimated as ±0.05 ML. TPD measurements provide a second measure of relative coverage for D_2O, which desorbs intact.[10]

LEED patterns were recorded using two different sets of LEED optics, a standard VG optics and florescent screen and an OCI system equipped with a dual channel plate detector. Since electron damage to the intact water structure is rapid (see below) several precautions were taken to minimize the electron dose during recording of LEED images using the standard optics. LEED images were recorded using a fast digital video camera at 6 frames s^{-1}, a typical drain current of 50 to 100 nA and a defocused electron beam spot, ~2 mm diameter, to minimize the electron dose. Images were recorded as electron exposure was initiated and the LEED patterns were visible in a single video frame, corresponding to an electron exposure of ~0.003 electron per adsorbed water. This allowed the LEED pattern to be monitored as a function of electron exposure in real time. A combination of LEED and post exposure TPD was used to reveal when the electron beam had caused damage to the surface. Damage was checked by moving to a new patch on the surface and by recording the TPD of the film after electron exposure from the LEED beam. Partial dissociation of D_2O forms a mixed $D/OD/D_2O$ phase which desorbs 33 K higher in temperature than the intact phase.[10] Once the time taken for electron damage to begin to modify the LEED pattern has been established, the LEED beam was scanned across the surface and individual frames averaged together to improve the noise levels as necessary. All measurements were repeated using the dual channel plate system (OCI) at a beam current <5 nA ($<10^{-4}$ electron/water per frame). In this case no electron beam damage was observed, even after extended exposure, and the LEED patterns were identical to the original results.

Reflection absorption IR spectra (RAIRS) of H_2O and D_2O structures were recorded using three different detectors, a narrow band InSb detector (5000–2000 cm^{-1}) optimized for the OH stretching region and two broadband MCT detectors (4000–670 and 4000–580 cm^{-1}) which were used for H_2O and D_2O, respectively. The broadband detector allowed the relative intensity of all three spectral regions [the OH(OD) stretch, the molecular scissors and the low frequency, out of plane librations] to be observed simultaneously, allowing conclusions to be drawn regarding the clustering and hydrogen bonding structure of the adsorbate. RAIRS were recorded both using molecular beam dosing (which gave a smaller surface spot and reduced signal to noise) and background adsorption (which gave better signal to noise but reduced isotopic purity and less precise control of the coverage) with consistent results. All spectra have been background corrected for reflectivity changes caused by

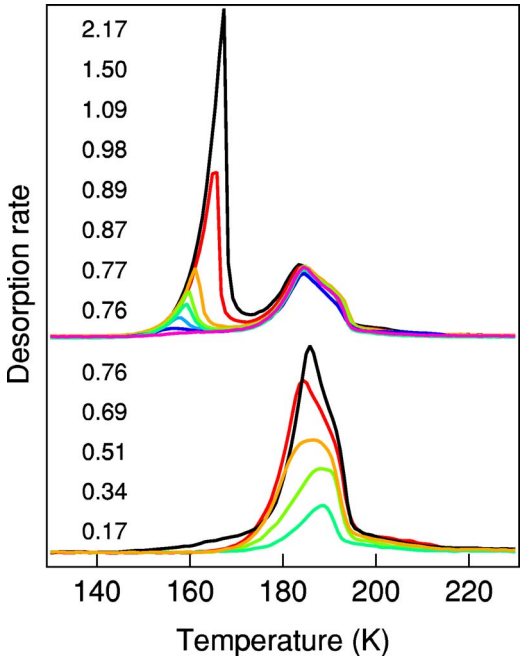

FIG. 1. (Color online) TPD of D_2O as a function of coverage after adsorption at 155 K (lower frame) and at 148 K (upper frame).

water adsorption and small changes in temperature. Throughout the text the word "water" is used only when the statement refers equally to H_2O or D_2O.

III. RESULTS AND DISCUSSION

A. LEED and RAIRS of adsorbed water

Water was adsorbed at temperatures $(140 \leqslant T \leqslant 160$ K) where it is mobile on the surface and forms hydrogen bonded structures, but does not dissociate.[10] Whereas H_2O undergoes partial dissociation as the surface is heated, forming a stable mixed $H/OH/H_2O$ phase which is seen as a second, high-temperature desorption feature,[10] isotopicly pure D_2O desorbs intact near 190 K, Fig. 1. The surface coverage was controlled by varying the exposure time and surface temperature. Figure 1 shows the desorption of D_2O as a function of the initial coverage following monolayer adsorption at 157 K (bottom frame), where adsorption saturates and no more uptake will occur, and at 150 K or below to form multilayers (top frame). At low coverage the first layer desorption peak stays at approximately the same temperature, before broadening and shifting to slightly lower temperature as the coverage is increased towards 0.69 ML. The desorption peak shape is quite different from the simple zero order desorption kinetics seen on Pt(111),[19] where water adsorbs and desorbs via a precursor mechanism and aggregates into extended, ordered hydrogen-bonded islands even at very low coverage, indicating a more complex growth/desorption behavior on Ru(0001).

As the first layer approaches saturation, a low-temperature tail forms and the main peak shifts back fractionally to higher temperature. Although the TPD traces indicate that this additional water is less stable than at coverages below 0.67 ML, this tail does not continue to grow, irrespective of the D_2O exposure. It is therefore not associated with growth of bulk ice multilayers, a conclusion reinforced by the LEED observations (see below). Only when the surface temperature is dropped below 150 K (for this particular gas flux) does a multilayer grow, with a distinct desorption peak some 30 K lower in temperature. Desorption of the multilayer film shows zero order desorption kinetics and its growth and structure is discussed in detail elsewhere.[20] Stabilization of water adsorbed in the first layer, compared to the multilayer, is clear evidence that water wets the Ru(0001) surface, contrary to the conclusions of DFT calculations based on a bilayer ice structure.[3] An identical low-temperature desorption tail is seen with H_2O,[10] both surfaces saturating with a coverage of 0.76 ± 0.05 ML, significantly more than the 0.67 ML expected for a $(\sqrt{3} \times \sqrt{3})R30°$ structure.

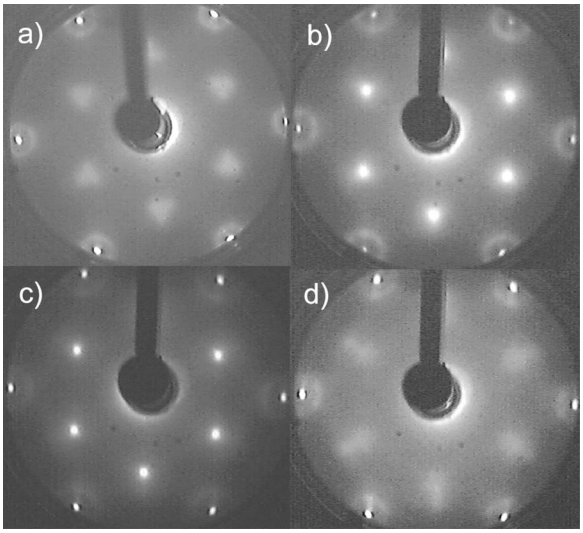

FIG. 2. LEED patterns for H_2O adsorbed on Ru(0001) at 155 K. (a) 0.29 ML, (b) 0.48 ML, (c) 0.67 ML, and (d) 0.76 ML. At the same coverage H_2O and D_2O LEED patterns are identical. Electron energy 54 eV.

When water is adsorbed at 155 K we observe formation of a $(\sqrt{3} \times \sqrt{3})R30°$ LEED pattern for both H_2O and D_2O adsorption, Fig. 2. This is contrary to the previous results of Held and Menzel,[21] who did not see a $\sqrt{3}$ pattern for H_2O but consistent with the original reports of Thiel *et al.*[11] and Doering and Madey.[12] For both H_2O and D_2O damage to the adsorbed layer by exposure to the electron beam (VG optics) could be followed by watching the degradation of the $\sqrt{3}$ LEED spots and development of a streaked LEED pattern when the adlayer was warmed above 140 K, Fig. 3. This LEED pattern is similar to that formed during dosing of H_2O at $T > 160$ K [Fig. 3(a)] or annealing a saturated H_2O layer to desorb the $A2$ feature[10] and has been reported earlier.[12,21] This structure is attributed to partial dissociation of water to form a mixed $H/OH/H_2O$ structure.[10] For D_2O electron damage could also be observed by the development of the high-temperature desorption feature due to mixed $D/OD/D_2O$ structures (Fig. 4) which is otherwise absent from the TPD of intact D_2O.[10] The effect of electron expo-

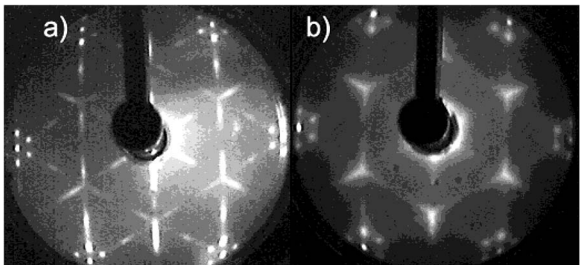

FIG. 3. LEED of (a) H_2O adsorbed at 165 K and (b) after exposing 0.48 ML film to electron damage and annealing to 150 K.

sure was minimized as described in Sec. II, allowing us to record LEED images free from electron damage. Measurements using the OCI low current LEED system gave identical results with no electron damage observed even after extended exposures, allowing us to obtain LEED images during isothermal annealing or desorption experiments.

As the water coverage is increased the $\sqrt{3}$ LEED spots remain diffuse, sharpening and becoming intense only as the water coverage approaches 0.6 to 0.67 ML. Again, this behavior is quite different to that seen for water adsorption on Pt(111), where formation of large islands of ordered ice result in a sharp $(\sqrt{37}\times\sqrt{37})R25°$ LEED pattern even at very low coverage,[19] Fig. 5. Weak arcs are visible around the Ru spots at low coverage, vanishing as the coverage approaches 0.6 ML. As the coverage on Ru(0001) is increased towards 0.67 ML (determined from the uptake measurements) the $\sqrt{3}$ spots become intense. As water adsorption continues beyond 0.67 ML the $\sqrt{3}$ LEED pattern becomes weaker and a ring reappears around the Ru spots, becoming larger in diameter as the coverage increases and then forming a sharp hexagon of spots as the surface saturates, Fig. 6(a). This superstructure hexagon is rotated 30° with respect to the (1×1) Ru spots and was also observed by Doering and Madey under conditions where we expect their film should be ordered but still intact [Fig. 6(c) (Ref. 12)]. This superstructure is distinct from that seen for the partially dissociated phase, Fig. 3,

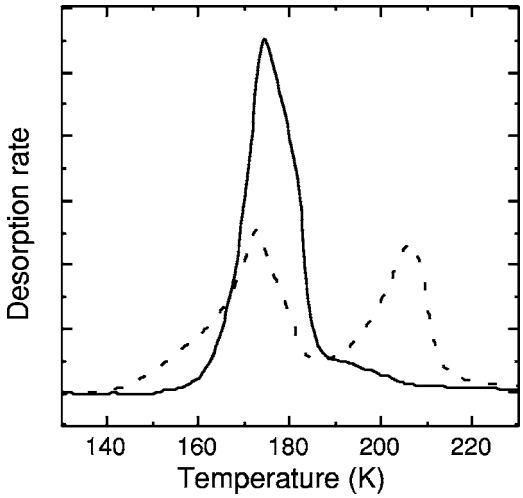

FIG. 4. TPD of pure D_2O (solid line) and after extended electron exposure from the LEED gun (approximately 2 electrons/water) (dotted line).

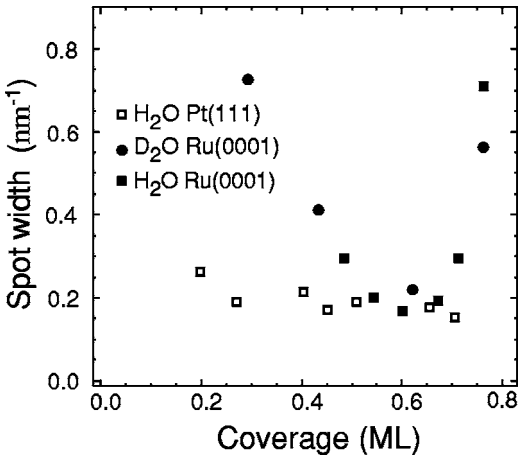

FIG. 5. LEED spot widths for the $(\sqrt{3}\times\sqrt{3})$ water structures on Ru(0001) (solid symbols) compared to the extended $(\sqrt{37}\times\sqrt{37})$ islands formed on Pt(111) (open symbols).

disappearing reversibly as water is desorbed from the surface at temperatures where the partially dissociated phase is stable. This distinction between the intact and partially dissociated phases was not clear in the earlier work.[12] The additional structure, the weakening and disorder of the $\sqrt{3}$ spots and the observation that adsorption saturates at a water coverage above 0.67 ML (Fig. 1), all indicate that adsorption does not saturate with a simple $(\sqrt{3}\times\sqrt{3})R30°$-$2H_2O(D_2O)$ layer. Instead additional water is present in the saturation adlayer, maximising the number of molecules in contact with the metal surface but disrupting the $(\sqrt{3}\times\sqrt{3})R30°$ order. The final density of water adsorbed on the Ru(0001) surface is 0.76 ML, 13% greater than in a hexagonal $(\sqrt{3}\times\sqrt{3})R30°$ structure and 8% greater than in an ideal bulk ice Ih bilayer. From the (00) satellite spots we find a superstructure periodicity of $\sim 8a_0$, very similar to the repeat length found by Doering and Madey.[12] The broadened $\sqrt{3}$ spots persist as a second water layer is grown on top of this structure, but are weak and the superstructure around the Ru spots becomes less well defined, Fig. 6(b). Ice layers of three layers or more, grown at $\leqslant$148 K, showed no LEED pattern.

In some of the LEED images an additional structure is observed as a faint, diffuse hexagonal structure, rotated 30° from the water pattern just inside the (2×2) positions. The

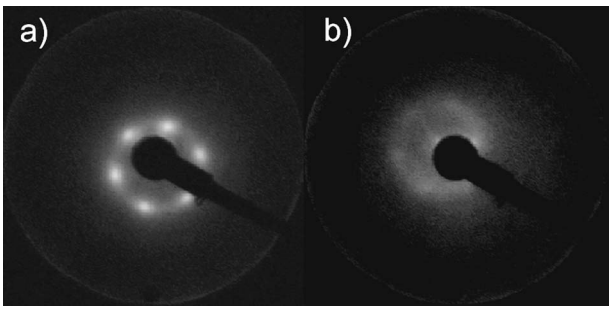

FIG. 6. Additional structure appearing around the Ru (00) spot, (a) at saturation and (b) for two layers of D_2O, 10 eV and 1 nA. The hexagon is oriented in the same direction as the first order Ru(0001) spots, which also display the same superstructure.

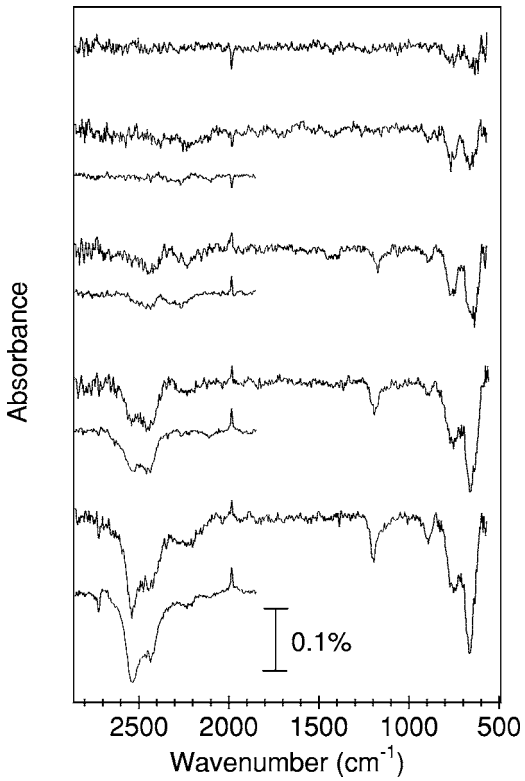

FIG. 7. RAIRS for D_2O adsorbed at 153 K as a function of coverage (0.05, 0.18, 0.44, 0.57, 0.70 ML). The spectra were recorded during slow film growth using an averaging time of 60 s. Spectra spanning 3000 to 1800 cm^{-1} were taken using a narrow band InSb detector and the others with a broadband MCT detector (3000–500 cm^{-1}). The spectra show bands in three regions, the OD stretch between 2200 and 2723 cm^{-1}, the DOD bend (scissors) at 1200 cm^{-1} and out of plane bending (librational) bands at 667, and 732 cm^{-1}. The feature near 900 cm^{-1} is due to a small amount of H_2O displaced from the wall and adsorbed on the surface during dosing.

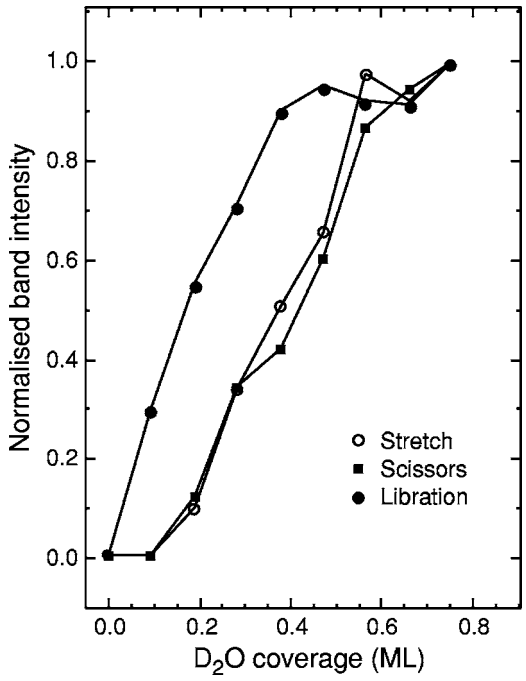

FIG. 8. Integrated intensities of the stretching, molecular scissors and libration bands recorded as a function of D_2O exposure during growth of a crystalline layer on Ru(0001) at 155 K.

additional spots appear only near 48 eV and were difficult to quantify, being variable in intensity. There was no evidence that these features changed with coverage, or became more pronounced during multilayer growth, suggesting that they are probably not associated with traces of second layer water. It seems possible that this pattern is due to a weak additional ordering of the $\sqrt{3}$ ice domains, or domain boundaries. Coadsorbed CO is known to interact strongly with water on Ru(0001), forming a (2×2)-$(2CO+D_2O)$ structure,[22] and it is also possible that this diffuse structure is due to traces of CO displaced from the chamber walls by water.

IR spectra of D_2O adlayers grown at 153 K are shown in Fig. 7 and show bands in the OD stretching region, extending from the free OD stretch at 2723 down to ~2100 cm^{-1}, the DOD scissors near 1200 cm^{-1} and out of plane librations of the hydrogen bonded water at 732 and 667 cm^{-1}. H_2O results in similar bands but with less defined structure in the OH stretching region [e.g., Fig. 2(a) (Ref. 10)]. Recording RAIR spectra during growth allows the intensities of different bands to be compared unambiguously. Although the signal to noise ratio of the spectra can be improved by averaging for longer times, slower dosing and longer averaging times allow small temperature changes to modify the reflectivity of the sample. While these can easily be removed for sharp absorption bands, distortion of the background is difficult to remove from the broad OH(OD) stretching bands. Based on the RAIRS of a complete $\sqrt{3}$ layer, we estimate the error on the intensity of the D_2O stretching, scissors and libration bands in Fig. 8 as 6, 11, and 4 % of saturation respectively, using the broadband detector. Although the signal to noise is a factor of 4 higher for the stretching bands recorded using the narrow band detector, the error on the band intensity is similar. In practice, changes to the orientation of water change the water detection sensitivity at low coverage, as discussed below.

As water is adsorbed two libration bands at 669 and 741 cm^{-1} appear immediately and persist to saturation, indicating that hydrogen-bonded D_2O structures are formed even at very low coverage. This is consistent with the expectation that water is mobile on the surface at these temperatures, and desorbs rapidly unless incorporated into a hydrogen-bonding network. As the coverage is increased further the D_2O scissors and OD stretching bands appear. Broad bands appear near 2106, 2267, and 2441 cm^{-1} which then develop into two strong bands near 2432 and 2538 cm^{-1}, with additional low-frequency structure. The free OD stretch appears at 2723 cm^{-1} only as the coverage approaches completion of the monolayer, with the OD stretch forming a broad structured band with intensity from 2600 down to ~2100 cm^{-1}. There is no evidence for the formation of well resolved, sharp stretching bands as observed during low temperature (20 K) adsorption[23] on this and other metal surfaces and for the proton ordered (3×3)-$2(OH+H_2O)$ structure on Pt(111).[24]

The RAIR spectra show several features which distinguish the water/Ru(0001) system from other observations of

ice films adsorbed on metal surfaces. Firstly the intensity of the OD stretch and scissors bands show a very different coverage dependence from that of the low-frequency libration modes associated with the out of plane bend of the hydrogen bonded water network, Fig. 8. This behavior persists in all the adsorption runs we made, both with D_2O and H_2O, although there were minor changes in the coverage at which the stretching bands appear (this appears to be sensitive to growth rate and temperature, for example the free OD stretch is more intense when the films are grown fast, or at lower temperatures). Since, ignoring any vibronic coupling to the substrate, the transition moment for the water stretch and scissors modes lies in the molecular plane, whereas that for the librations lies perpendicular to the OH-O bond, the change in relative intensity of the stretch/scissors and librational bands suggests a change in the orientation of water as the coverage increases. At low coverage water lies flat, making the OD stretch and scissors dipole forbidden and therefore weak in the RAIR spectrum. As the coverage increases the ice restructures, some of the water moves into a buckled geometry and the OD stretch and scissors bands become strong.

There are two other notable differences between the intact monolayer on Ru(0001) and the RAIR spectrum of other water films. The high-frequency "free" OH(OD) band at 3683(2723) cm^{-1}, which is associated with OH which has no hydrogen bonding, is weak and has an intensity which depends on the exact preparation of the overlayer. Provided the film is grown slowly, at a sufficiently high temperature to allow good annealing, the band only becomes visible at coverages above 0.67 ML as the water monolayer saturates. In systems where some water is adsorbed H-up, such as on Cu(110),[25] this band is intense. Denzler *et al.*[5] also find this feature is weak in SFG, appearing as the multilayer starts to form. Free OH/OD appears to be associated not with the ordered $(\sqrt{3}\times\sqrt{3})R30°$ lattice formed at coverages up to 0.67 ML, but with a minority species formed as the $\sqrt{3}$ structure compresses towards its saturation coverage of 0.76 ML. Our conclusion is that the $(\sqrt{3}\times\sqrt{3})R30°$ ice structure does not contain free OH/OD dangling into the vacuum but has water adsorbed flat or H down. Free OH/OD is only formed as a minority species in the structure as the monolayer compresses to saturation. Finally, the OD stretching bands on Ru(0001) are broader than seen for thin films of crystalline D_2O,[26] or for a D_2O monolayer adsorbed on Pt(111),[19] where the stretching band does not extend below $\sim$2200 cm^{-1}. The presence of low-frequency bands is particularly noticeable at low coverage, but absorption in this range persists at higher coverage, as the higher-frequency absorption becomes intense. The reduced frequency of the OD absorption band at low coverage is probably associated with a softened OD stretch due to a strong interaction between Ru and water adsorbed in small clusters, flat on the surface in its optimum binding geometry. We also note that low frequency absorption in hydrogen bonded systems can be associated with particularly short O-O separations in the hydrogen bonded film, following the correlation between the OD stretching frequency and the O-O separation in hydrogen-bonded ice structures recently highlighted by Feibelman.[9] This issue will be discussed further in Sec. IV.

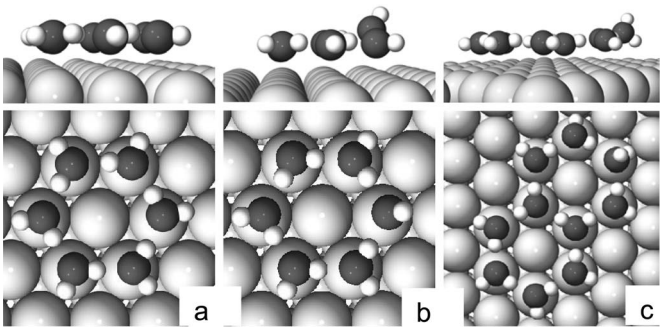

FIG. 9. (a) Optimum adsorption geometry for a hexamer of water on Ru(0001). Water sits flat on the surface with O almost coplanar ($\Delta z \leq 0.06$ Å) atop Ru, with a Ru-O separation of 2.43 Å. (b) Water hexamer in which a water has both protons hydrogen bonded in the ring. (c) Double ring showing the growth of a second ring from the planar nucleus shown in (a).

Water monomers prefer to adsorb flat, atop a Ru atom,[3,7,27] but the binding energy is low and adsorption is stabilized only by hydrogen bonding. Formation of small hexamers has been observed on other surfaces [e.g., Ag(111) (Ref. 28)] and allows water to gain two hydrogen bonds without necessarily having to forfeit its planar adsorption geometry. A similar preference for water to bind flat has recently been associated with formation of defective $\sqrt{3}$ structures during water adsorption on Pd(111).[29] The observed LEED and RAIRS behavior during adsorption can be understood in terms of a change from a flat geometry in small clusters of water, with poor long range lateral ordering of the adsorbate, to an extended commensurate buckled structure as the coverage approaches 0.67 ML. This complete structure has a $(\sqrt{3}\times\sqrt{3})R30°$ LEED pattern and has water adsorbed flat or OH/OD down. As the monolayer completes more water is incorporated into this structure, disordering the structure and resulting in the growth of the free OH/OD band.

B. Density functional theory calculations

In order to test this model we carried out DFT calculations using VASP (Refs. 30 and 31) to examine the structure and binding energy of water clusters and different water adlayers on Ru(0001). Standard ultrasoft pseudopotentials and the PW91 version of generalized gradient approximation[32] were used with a plane wave energy cutoff of 29.1 Ry. The surface was represented by three layers of Ru, with the experimental lattice constants, and a vacuum gap of 16 Å. The bottom two layers were fixed in the bulk lattice positions and all other atoms were relaxed until no force component was larger than 0.03 eV/Å. All calculations used a $3\times3\times1$ Monkhorst-Pack *k*-point set[33] with a $2\sqrt{3}\times2\sqrt{3}$ unit cell, except for those on "isolated" hexamers and the double ring, Fig. 9, for which we used a (4×4) or $(5\times\sqrt{13})$ unit cell.

The results for intact $(\sqrt{3}\times\sqrt{3})R30°$ bilayers are similar to those found earlier,[3,7] Table I, with only a small difference between the binding energies for water adsorbed in the H-up

TABLE I. Binding energies (ΔE_{ads}) and range of O-O separations ($R_{O\text{-}O}$) of water adsorbed in different structures.

Structure	ΔE_{ads} (eV)	$R_{O\text{-}O}$(Å)
H-up bilayer	0.562	2.76, 2.86
	0.52,[a] 0.58,[b] 0.54,[c]	
	0.53,[d] 0.58,[e]	
H-down bilayer	0.527	2.75, 2.81
	0.53,[a] 0.57,[b] 0.50,[c]	
	0.53,[d] 0.58[e]	
Flat hexamer	0.594[f]	2.69–2.71
Buckled hexamer	0.578[g]	2.61–2.82
Double ring	0.601[h]	2.66–2.86
Chains	0.658[i]	2.67–2.87
Short chains	0.625[j]	2.61–2.91

[a]Ref. 3.
[b]Ref. 7.
[c]Ref. 4.
[d]Ref. 38.
[e]Ref. 45.
[f]Fig. 9(a).
[g]Fig. 9(b).
[h]Fig. 9(c).
[i]Fig. 10(a).
[j]Fig. 10(b).

and H-down bilayer structures. The omission of dispersion forces in these calculations means that the binding energies are expected to be too low[34] and we should be careful in considering such small differences as significant. As a result DFT can probably not be used to distinguish which of these structures is favored. However, as Feibelman originally pointed out, the binding energy of the bilayer structures is significantly less than that calculated under the same conditions for bulk ice (~0.67 eV) or the experimental lattice energy of 0.61 eV. The conclusion from DFT is that a conventional H-up or H-down bilayer should not wet the Ru(0001) surface.[3] Since this is in conflict with the emerging experimental consensus that water remains intact below 155 K and wets the Ru(0001) surface,[10,16] either DFT is simply inadequate to calculate the energetics to the required accuracy and dispersion forces must be included,[34] or the structure of the wetting layer is different from the bilayer assumed previously.[12]

Since stable hexamers have been seen on other metal surfaces at low coverage,[28] we investigated the binding energy and structure of small clusters on Ru(0001). We find that water hexamers are significantly more stable than the complete ice bilayer, with a binding energy of 0.594 eV (Table I), despite having just two hydrogen bonds per water molecule compared to three in the bilayer. The most stable water cluster we found is the symmetric hexamer, shown in Fig. 9(a), with each water adsorbed atop Ru, parallel to the surface with one H atom pointing out of the ring. In the absence of vibronic coupling, the planar water geometry will result in the in-plane water scissors and OH stretching modes being weak (dipole forbidden) and just the out-of-plane libration

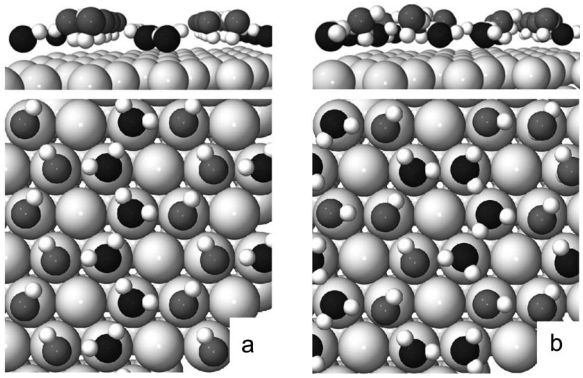

FIG. 10. Structure of a complete hexagonal water overlayer calculated in a $(2\sqrt{3}\times 2\sqrt{3})$ unit cell. O atoms lying closest to the surface are shaded dark. (a) "Chain" structure showing water adsorbed "flat" ($R_{O\text{-}Ru}$=2.36 Å) or "H-down" ($R_{H\text{-}Ru}$=2.43 Å and $R_{O\text{-}Ru}$=3.39 Å) in extended chains with a $(\sqrt{3}\times 2\sqrt{3})$ periodicity. The flat waters have one H directed in plane along the chain and one tilted up towards the neighboring H-down chain. (b) One of three non-trivially related "short chain" structures with a $(2\sqrt{3}\times 2\sqrt{3})$ periodicity. The hydrogen bond distances within the flat chains are 1.61, 1.68, and 1.72 Å, compared to 1.97, 1.85, and 2.08 Å within the H-down chains.

strong, as observed in RAIRS at low coverage (Fig. 7). If one of the water molecules is chosen to have both H atoms hydrogen bonded to another water in the ring [Fig. 9(b)], another water is forced to sacrifice its planar geometry, buckling out of plane. The binding energy of the cluster is reduced by 0.1 eV, some 20% of a water molecule's binding energy, indicating a clear preference for water to retain its flat adsorption geometry on Ru(0001). The growth of small clusters [Fig. 9(c)] allows additional hydrogen bonding (Table I) but requires at least one water in each additional ring to buckle out of plane. As the clusters grow larger more water is forced to lose its planar geometry, destabilizing the cluster. As water buckles out of plane the stretch and scissors bands become dipole active, resulting in the increase in intensity of these bands observed experimentally at higher coverage.

The LEED patterns of both H_2O and D_2O indicate a well ordered $(\sqrt{3}\times\sqrt{3})R30°$ structure forms as the water coverage approaches 0.67 ML. Since LEED is sensitive only to the O and Ru positions, we looked for stable hydrogen bonded structures with larger unit cells which retain the hexagonal, honeycomb O backbone but have a different proton ordering. The effect this will have on the LEED patterns and RAIR spectra is discussed later. For conventional water bilayers the H-down structure had the lowest binding energy, 0.527 eV (Table I) but this increases slightly to 0.562 eV for the "H-up" structure, and 0.564 eV for mixed "H-up/down" bilayer structures. Abandoning the conventional bilayer model, and assuming that water prefers to retain a flat lying geometry, resulted in the structure shown in Fig. 10(a). This structure has a binding energy of 0.658 eV (Table I), some 100 meV larger than for a conventional bilayer. The work function of this structure is calculated to be 1.15 eV, compared to the 1.3 eV observed experimentally.[21] Unlike the ice bilayer model, this structure does not have water alternating between

the upper and lower bilayers, instead water is arranged into chains of molecules bound nearly "flat" on the surface, linked to "upright" chains which are bound to Ru H-down. Each flat lying or upright water has hydrogen bonds to two neighbors in the chain, which have a similar geometry, and one linking to water in a neighboring chain adsorbed with the other geometry. The hydrogen bonds along the flat water chains are short (1.70 Å), while the H-down chains are tilted over to give 1.80 Å bonds to the flat water chains—at the expense of leaving long hydrogen bonds (1.91 Å) between the H-down waters. Top layer Ru atoms bound to the flat water chains are displaced 0.06 Å towards the vacuum. The corresponding chain structure with water chains adsorbed flat and H up, with OH dangling into the vacuum, is not stable. This is consistent with our conclusion from RAIRS that water is adsorbed H down.

The stability of this chain structure compared to a conventional ice bilayer presumably originates from the ability of half the water to adsorb close to Ru in its preferred flat atop adsorption geometry, while still maintaining a complete hydrogen bonding network. By contrast, in the conventional bilayer each water is hydrogen bonded to three neighbors in the other half of the bilayer, requiring water adsorbed on Ru either to sacrifice its favored planar geometry in favor of optimising hydrogen bonding in the bilayer, or to adsorb flat and compromise the hydrogen bond to the upper bilayer. Since the bilayer structure of ice Ih(0001) is imposed by the tetrahedral distribution of the four hydrogen bonds around water in bulk ice, there is no obvious reason why this should be preserved for a 2D ice monolayer at the Ru(0001) surface.

As well as the chain structure of Fig. 10(a), which has a $(\sqrt{3}\times 2\sqrt{3})R30°$ repeat, we looked for other stable hexagonal, 2/3 ML structures in the $(2\sqrt{3}\times 2\sqrt{3})$ unit cell. Figure 10(b) shows a "short chain" structure containing chains of flat and upright water molecules four molecules long in a $(2\sqrt{3}\times 2\sqrt{3})R30°$ arrangement. This structure is associated with a reduction in the number of hydrogen bonds between water molecules in the same geometry (flat or H down), each water at the end of a chain having two hydrogen bonds to the opposite chain. Although this arrangement leaves half the water molecules binding to two molecules with the opposite adsorption geometry, it still avoids the situation where each water is surrounded by three molecules of a different orientation, as found in the conventional bilayer structure. The binding energy of the short chain structure shown in Fig. 10(b) is 0.625 eV, only slightly lower than that of the extended chains and still significantly more stable than the conventional bilayer. The hydrogen bond distances within the flat chains are short, 1.61, 1.68, and 1.72 Å, compared to 1.97, 1.85, and 2.08 Å within the H-down chains. The arrangement shown in Fig. 10(b) is the structure which evolves during energy minimisation starting from a network of flat water hexamers linked into a complete structure by upright bridging waters.

The chain structures shown in Fig. 10 represent only two of many possible structures which can be formed for a honeycomb network of water containing chains of flat and H-down water. The "long chain" structure [Fig. 10(a)] can be modified in several ways without introducing any terminating defects into the chains or significantly changing the water binding energy. The proton alignment of adjacent chains can be switched independently of each other, giving two non-equivalent structures with a $(\sqrt{3}\times 2\sqrt{3})$ repeat as well as further structures of the type $(\sqrt{3}\times 2n\sqrt{3})$. The chain direction can be changed from $\langle 1\bar{2}1\rangle$ to $\langle 2\bar{1}\bar{1}\rangle$ or $\langle \bar{1}\bar{1}2\rangle$ at any point down a chain, requiring only a different choice of the two (equivalent) directions for the next unit. Instead of forming chains along the $\langle 1\bar{2}1\rangle$ directions the same flat and H-down units can be used to build zig-zag chains along the close packed directions, again without introducing any water molecules with a different number of flat and H-down neighbors. For short chains the number of possible configurations are even larger, the short chain structure of Fig. 10(b) having three possible non-equivalent proton arrangements even before different unit cells are considered. Choosing larger unit cells allows many different structures to be formed, containing flat and H-down chains two or more units long, with different local proton orientations and a broad range of O-O separations. Since the energy cost of creating the flat/H-down chain termination is low, these structures are likely to play an important role for real adlayers where limited mobility during growth of the film will freeze disorder into the structure.

The model which emerges from this interpretation of the DFT calculations is of water adsorbed in a well defined honeycomb structure atop Ru, containing water arranged in chains with a flat and H-down geometry. Unlike the rigid alternation in water geometry intrinsic to the bilayer model, formation of chains is expected to give substantial disorder in the ice structure, associated with the proton orientation along the chains, the direction of the chains and their length. The hydrogen bonding network gives rise to a strong long-range order in the lateral location of the water, producing a well defined $(\sqrt{3}\times\sqrt{3})R30°$ periodicity in the O location. In contrast the water orientation (flat or H down) is expected to show a short-range preference to have two neighbors of the same orientation, but no long-range order in either the water orientation or the O height. A direct experimental test between the bilayer and chain model proposed here requires a probe of the local O coordination geometry which is not yet available. Below we discuss the existing experimental evidence about the structure of intact water on Ru(0001) and its consistency with the chain structure found in DFT.

IV. DISCUSSION

The RAIRS and LEED results for water adsorption presented above were made at temperatures where water is mobile and can diffuse to form stable hydrogen bonding structures on the surface. The ice film initially grows as clusters or $(\sqrt{3}\times\sqrt{3})R30°$ islands, with water preferentially adsorbed flat, with limited long-range order, Fig. 2. Only as the film approaches 0.6 to 0.67 ML coverage does it form large extended islands of ice, the intensity of the OH/OD stretching bands increasing as the structure buckles to make the stretching bands dipole active, Figs. 7 and 8. A recent IR study of water on Ru(0001) shows the D_2O scissors disappearing as

the ice is annealed from 25 to 162 K at low coverage,[35] consistent with the water moving into a flat lying cluster geometry on annealing. A similar coverage dependence to the intensity of the OH stretching bands was observed for water adsorbed on Ni(110) (Ref. 36) and attributed to adsorption of water flat on the surface. The RAIRS behavior is consistent with the observation of stable, flat lying water hexamers in DFT (Fig. 9). Aggregation of ice clusters into a continuous network may be inhibited either by the decrease in binding energy associated with rotation of water out of plane as the clusters grow, or kinetically by the need to reorient water from flat to H down to form extended ice clusters. This preference for water to remain flat is similar to the behavior on Pd(111) where, under conditions of limited mobility, water forms defective lace structures to maximize the number of waters adsorbed flat.[29]

The absence of a free OH/OD stretch at coverages of 0.67 ML or less in RAIRS, as in SFG,[5] is consistent with water being adsorbed flat or H-down in the ice layer until after the 0.67 ML $(\sqrt{3}\times\sqrt{3})R30°$ structure is completed. This is the same geometry favored for water on Pt(111),[37] where no free OH/OD band is seen in RAIRS,[19] whereas water forms a mixed H-up/H-down structure on Cu(110) with a prominent free OH/OD peak.[25] Water adsorbed H-down does not appear as a sharp high-frequency band, presumably a result of coupling to the metal broadening and redshifting these bands to lower frequency. As adsorption continues additional water is incorporated into the $(\sqrt{3}\times\sqrt{3})R30°$ layer, weakening the $\sqrt{3}$ LEED pattern (Fig. 2) and forming minority H-up water which is visible as the sharp free OH/OD band in RAIRS, Fig. 7. The compression of the ice layer that occurs as it approaches saturation will influence the growth of crystalline ice multilayers on this wetting layer.[20]

Although the $\sqrt{3}$ spots become much weaker, the saturation layer shows evidence of a long-range $8a_0$ repeat associated with compression of the $\sqrt{3}$ structure to accommodate more water. The saturation coverage of $0.76\pm.05$ ML is inconsistent with formation of a uniformly compressed hexagonal structure with this (approximate) periodicity, while the absence of sharp higher order LEED spots indicates that the surface does not form a regular hexagonal network akin to the $(\sqrt{37}\times\sqrt{37})R25°$ and $(\sqrt{39}\times\sqrt{39})R16°$ structures seen on Pt(111).[19] The saturated phase probably consists of high density domain boundaries in an H-down $\sqrt{3}$ structure, with some of the additional water adsorbed H up. This is similar to the picture originally suggested by Doering and Madey[12] who proposed an ordered array of antiphase domains with a $5(\sqrt{3}\times\sqrt{3})$ spacing. This arrangement results in a coverage of 0.78 ML, very close to the value 0.76 ML found here. The formation of an H-down structure with upright water present only as a minority species as the film compresses also helps to explain the weak axial ESDIAD peak observed at saturation,which was in fact originally attributed to a dislocation structure.[12] At lower coverage a hexagonal ESDIAD pattern forms, with emission along the Ru close packed directions. This pattern is consistent with proton emission from minority water species adsorbed at the edge of clusters with one H pointing up in the tilted geometry shown in Figs. 9(b) and 9(c). Although this explanation is similar to that proposed originally, based on proton emission from water adsorbed at the edge of islands with just one hydrogen bond to a cluster and H pointing up along the close packed directions,[12] this latter adsorption geometry is not consistent with the preference for water to adsorb flat and to form at least two hydrogen bonds.

Recently Meng *et al.*[38] proposed that the SFG spectrum and work function of the $(\sqrt{3}\times\sqrt{3})R30°$ ice film could be explained by a bilayer containing a mixture of H-up and H-down water. The work function of the ice film [$\Phi=1.3$ eV (Ref. 21)] rules out the partially dissociated structure ($\Phi=0.3$ eV) and was interpreted as a mixture of the H-up ($\Phi=3.0$ V) and the H-down structure ($\Phi=0.4$ eV) in an appropriate ratio. While entropy effects favor a disordered H-up/H-down water bilayer, these are small ($\sim$9 meV/molecule) and can make only a minor contribution to the free energy.[39] This means that the H-up and H-down structures must (quite by chance) have identical binding energies to support a mixture of the two geometries. Meng *et al.* suggested that the absence of a free OH stretch might be explained on the basis of phase cancellation in the SFG signal between H-up and H-down bands. Although this explanation seems unlikely, since we must expect the frequency of the H-up and H-down species to differ slightly, it can anyway be excluded from the absence of any free OH/OD signal in RAIRS before the $\sqrt{3}$ phase starts to compress, Fig. 7. The chain structure (Fig. 10) has a work function $\Phi=1.15$ eV which is very close to the 1.3 eV observed experimentally and is also consistent with the absence of free OH/OD in the RAIRS spectrum. Here we discuss whether this structure is consistent with other experimental observations of water on Ru(0001).

Feibelman's original suggestion that water was partially dissociated on Ru(0001) (Ref. 3) was made to explain the wetting of this surface and the absence of an O buckling in the LEED IV analysis of the $(\sqrt{3}\times\sqrt{3})R30°$ D_2O structure.[13] The binding energy of the chain structure (Fig. 10) is 0.66 eV, 17% greater than the conventional H-up ice bilayer assumed in most previous work.[1] This is larger than the experimental ice binding energy (0.61 eV) and similar to that found by DFT for bulk ice [0.66 or 0.71 eV (Ref. 3)], suggesting that this structure will indeed wet the surface. There are two possible interpretations for the absence of an O corrugation in the LEED IV analysis. The first is that, despite the measures taken to avoid it, electron damage to the adlayer formed the partially dissociated structure.[40] Since calculations[3] indicate that O in this layer is coplanar, and RAIRS shows OH/H_2O is adsorbed flat on the surface,[10] this could explain the absence of any corrugation in the IV analysis. An alternative explanation can be made on the basis of the chain structure discussed above. Analysis of the LEED IV data assumed a simple $(\sqrt{3}\times\sqrt{3})R30°$ unit cell with the two distinct O atoms at different heights, associated with the lower and upper bilayer, and a buckling of Ru. However, the chain structures have no simple local $\sqrt{3}$ ordering of the flat or H-down water sites within the hexagonal superstructure. Although the chains (Fig. 10) have an O corrugation of 1 Å, this will not be properly represented in the LEED analysis.

Disorder in the flat/H-down chain direction and length will remove any long-range correlation between the height of adjacent O atoms, reducing the overall LEED pattern from the $(\sqrt{3}\times 2\sqrt{3})$ symmetry of the ideal chain structure [Fig. 10(a)] to that of the $(\sqrt{3}\times\sqrt{3})R30°$-O skeleton. Similarly, the absence of any correlation between the height of adjacent O atoms will mask the up/down O corrugation, irrespective of the degree of electron damage the film suffered, and may explain the rather large vibrational amplitude of O required to model the IV spectrum.[8]

This new model of the $\sqrt{3}$ ice structure also allows us to address the broad OH/OD stretching bands seen in RAIRS. The proton ordered $(OH+H_2O)$-Pt(111) layer shows sharp RAIRS bands at 3475(2570) cm^{-1} in the stretching region and a libration at 1015 (756) cm^{-1} with linewidths of just 35(12) cm^{-1}.[24,41] Similarly, small crystalline ice clusters show sharp features in their IR spectra.[42,43] When the proton order of the $(OH+H_2O)$-Pt(111) structure is removed by changing the H content slightly, a disordered system results with different local environments and the RAIRS bands broaden. Calculations of the vibrational spectrum of $(OH+H_2O)$ (Ref. 44) and of ordered intact $\sqrt{3}$ bilayers (e.g., Ref. 38) predict a number of bands across the stretching region. While in both cases inelastic coupling will broaden these bands, the breadth of the water bands observed experimentally suggests there must be some additional mechanism broadening the ice spectra. Unlike the ice bilayer model, the chain structures contain a range of O-O separations, between 2.61 and 2.91 Å for the structure shown in Fig. 10(b). On the basis of the strong correlation between the O-O separation and the OH(OD) stretching frequency,[9] we expect IR bands between ~2250 and 2550 cm^{-1}, as seen in RAIRS (Fig. 7). For larger unit cells a greater range of local water geometries will be possible, providing a further heterogeneous broadening to the RAIRS bands, over and above the inelastic coupling expected.

Finally, it is revealing to contrast the differing behavior of water adsorbed on the Ru(0001) and Pt(111) close packed faces. Whereas on Ru(0001) water initially forms flat lying clusters of water with little long range order, on Pt(111) it aggregates to form extended islands with a hexagonal honeycomb structure.[46,47] Vibrational spectroscopy shows no evidence for formation of flat water clusters, the stretching bands being visible even at low temperatures.[19,22,23] At low coverage the ice adopts a $(\sqrt{37}\times\sqrt{37})R25°$ registry, but the structure compresses at higher coverage to form a $(\sqrt{39}\times\sqrt{39})R16°$ phase.[19,46–48] In both of these structures water appears to sacrifice the favored atop Pt binding site in order to optimize the lateral density of the ice. In contrast on Ru(0001) water adopts a simple $(\sqrt{3}\times\sqrt{3})R30°$ network, allowing it to bond in the favored atop adsorption geometry.[3,13]

Calculations find that water monomers adopt a similar geometry on both surfaces, binding flat atop the metal to maximize overlap of the $1b_1$ orbital,[27] with a similar variation in binding energy with adsorption site. The binding energy of water on Ru is slightly greater than on Pt,[27] which will favor optimizing the water-metal interaction in the atop Ru site at the expense of compromising the hydrogen bonding network slightly compared to Pt. However, the difference in monomer binding energy is very small [0.38 and 0.35 eV for Ru and Pt, respectively (Ref. 27)] and the adsorption behavior is also affected by the lateral spacing. In order to form a $(\sqrt{3}\times\sqrt{3})R30°$ network the ice structure must match the Ru lattice parameter, which has a next-nearest-neighbor distance of 4.69 Å, 3.7% larger than the lateral repeat distance in ice Ih. The flat water hexamer on Ru(0001) [Fig. 9(a)] has an O-O bond length just 0.2% shorter than the Ru spacing, indicating that water adsorbed in flat chains (Fig. 10) has a lateral period very close to its optimal spacing. On Pt(111) the next-nearest-neighbor distance is 4.81 Å, 6.3% larger than the lateral repeat distance in ice Ih. Whereas the hexamer on Ru(0001) lies flat (Fig. 9), on Pt(111) we calculate a buckled structure with water adsorbed in two layers with an O corrugation of 0.69 Å and a binding energy of 0.52 eV. Formation of a buckled structure is consistent with the RAIR spectra and the absence of flat lying water clusters on Pt(111). The lateral position of O in this hexamer is contracted inwards from the Pt positions by 6%, giving a lateral period similar to that of bulk ice Ih. The increased lattice parameter of Pt shifts the energetic balance away from maintaining a flat atop adsorption geometry above the metal in favor of optimizing the hydrogen bonding structure and lateral spacing of the water layer. The result is a labile ice structure on Pt(111), capable of adopting a range of lateral densities in response to submonolayer or multilayer adsorption.[48]

V. CONCLUSION

On Ru(0001) water forms an intact film which is metastable with respect to a partially dissociated phase,[16] thermal dissociation showing a strong isotope effect.[10] Water adsorption creates flat lying clusters, rather than extended islands, preferring to optimize the Ru-water interaction at the expense of a reduced hydrogen bonding coordination. Only as the coverage increases towards 0.67 ML does the film order into a $(\sqrt{3}\times\sqrt{3})R30°$ structure, water buckling out of plane into an H-down geometry. DFT suggests that the complete adlayer probably does not adopt the ice bilayer structure assumed previously, instead forming disordered chains of water arranged in flat and upright H-down chains embedded in a hexagonal $(\sqrt{3}\times\sqrt{3})R30°$ superstructure. This structure appears to be consistent with the work function, RAIRS and other existing experimental data. Adsorption continues past the ordered 0.67 ML structure to saturate with a coverage of 0.76 ML, with some of the additional water adsorbed in an H-up geometry, probably at domain boundaries as originally suggested.[12]

ACKNOWLEDGMENTS

We would like to thank Werner Hofer for assistance with the DFT calculations and the EPSRC for support of this work.

[1] P. A. Thiel and T. E. Madey, Surf. Sci. Rep. **7**, 211 (1987).
[2] M. A. Henderson, Surf. Sci. Rep. **46**, 5 (2002).
[3] P. J. Feibelman, Science **295**, 99 (2002).
[4] A. Michaelides, A. Alavi, and D. A. King, Phys. Rev. B **69**, 113404 (2004).
[5] D. N. Denzler, C. Hess, R. Dudek, S. Wagner, C. Frischkorn, M. Wolf, and G. Ertl, Chem. Phys. Lett. **376**, 618 (2003).
[6] P. J. Feibelman, Phys. Rev. B **67**, 035420 (2003).
[7] A. Michaelides, A. Alavi, and D. A. King, J. Am. Chem. Soc. **125**, 2746 (2003).
[8] S. R. Puisto, T. J. Lerotholi, G. Held, and D. Menzel, Surf. Rev. Lett. **10**, 487 (2003).
[9] P. J. Feibelman, Chem. Phys. Lett. **389**, 92 (2004).
[10] C. Clay, S. Haq, and A. Hodgson, Chem. Phys. Lett. **388**, 89 (2004).
[11] P. A. Thiel, F. M. Hoffmann, and W. H. Weinberg, J. Chem. Phys. **75**, 5556 (1981).
[12] D. L. Doering and T. E. Madey, Surf. Sci. **123**, 305 (1982).
[13] G. Held and D. Menzel, Surf. Sci. **316**, 92 (1994).
[14] G. Held and D. Menzel, Phys. Rev. Lett. **74**, 4221 (1995).
[15] P. J. Schmitz, J. A. Polta, S. L. Chang, and P. A. Thiel, Surf. Sci. **186**, 219 (1987).
[16] K. Andersson, A. Nikitin, L. G. M. Pettersson, A. Nilsson, and H. Ogasawara, Phys. Rev. Lett. **93**, 196101 (2004).
[17] J. Weissenrieder, A. Mikkelsen, J. N. Andersen, P. J. Feibelman, and G. Held, Phys. Rev. Lett. **93**, 196102 (2004).
[18] J. Harnett, S. Haq, and A. Hodgson, Surf. Sci. **528**, 15 (2003).
[19] S. Haq, J. Harnett, and A. Hodgson, Surf. Sci. **505**, 171 (2002).
[20] S. Haq, C. Clay, and A. Hodgson (unpublished).
[21] G. Held and D. Menzel, Surf. Sci. **327**, 301 (1995).
[22] M. Nakamura and M. Ito, Surf. Sci. **490**, 301 (2001).
[23] M. Nakamura and M. Ito, Chem. Phys. Lett. **325**, 293 (2000).
[24] C. Clay, S. Haq, and A. Hodgson, Phys. Rev. Lett. **92**, 046102 (2004).
[25] T. Schiros, S. Haq, H. Ogasawara, O. Takahashi, H. Öström, K. Andersson, L. G. M. Pettersson, A. Hodgson, and A. Nilsson (unpublished).
[26] J. E. Schaff and J. T. Roberts, J. Phys. Chem. **100**, 14 151 (1996).
[27] A. Michaelides, V. A. Ranea, P. L. de Andres, and D. A. King, Phys. Rev. Lett. **90**, 216102 (2003).
[28] K. Morgenstern and J. Nieminen, Phys. Rev. Lett. **88**, 066102 (2002).
[29] J. Cerda, A. Michaelides, M. L. Bocquet, P. J. Feibelman, T. Mitsui, M. Rose, E. Fomin, and M. Salmeron, Phys. Rev. Lett. **93**, 116101 (2004).
[30] G. Kresse and J. Hafner, Phys. Rev. B **47**, 558 (1993).
[31] G. Kresse and J. Furthmuller, Phys. Rev. B **54**, 11169 (1996).
[32] J. P. Perdew, J. A. Chevary, S. H. Vosko, K. A. Jackson, M. R. Pederson, D. J. Singh, and C. Fiolhais, Phys. Rev. B **46**, 6671 (1992).
[33] H. J. Monkhorst and J. D. Pack, Phys. Rev. B **13**, 5188 (1976).
[34] P. J. Feibelman, Phys. Rev. B **72**, 113405 (2005).
[35] M. M. Thiam, T. Kondo, N. Horimoto, H. S. Kato, and M. Kawai, J. Phys. Chem. B **109**, 16024 (2005).
[36] B. W. Callen, K. Griffiths, and P. R. Norton, Phys. Rev. Lett. **66**, 1634 (1991).
[37] H. Ogasawara, B. Brena, D. Nordlund, M. Nyberg, A. Pelmenschikov, L. G. M. Pettersson, and A. Nilsson, Phys. Rev. Lett. **89**, 276102 (2002).
[38] S. Meng, E. G. Wang, C. Frischkorn, M. Wolf, and S. W. Gao, Chem. Phys. Lett. **402**, 384 (2005).
[39] P. J. Feibelman and A. Alavi, J. Phys. Chem. B **108**, 14362 (2004).
[40] N. S. Faradzhev, K. L. Kostov, P. Feulner, T. E. Madey, and D. Menzel, Chem. Phys. Lett. **415**, 165 (2005).
[41] G. Held, C. Clay, S. Barrett, S. Haq, and A. Hodgson, J. Chem. Phys. **123**, 064711 (2005).
[42] M. Nakamura, Y. Shingaya, and M. Ito, Chem. Phys. Lett. **309**, 123 (1999).
[43] M. Nakamura and M. Ito, Chem. Phys. Lett. **384**, 256 (2004).
[44] G. S. Karlberg, F. E. Olsson, M. Persson, and G. Wahnstrom, J. Chem. Phys. **119**, 4865 (2003).
[45] G. Materzanini, G. F. Tantardini, P. J. D. Lindan, and P. Saalfrank, Phys. Rev. B **71**, 155414 (2005).
[46] M. Morgenstern, J. Muller, T. Michely, and G. Comsa, Z. Phys. Chem. **198**, 43 (1997).
[47] A. Glebov, A. P. Graham, A. Menzel, and J. P. Toennies, J. Chem. Phys. **106**, 9382 (1997).
[48] G. Zimbitas, S. Haq, and A. Hodgson, J. Chem. Phys. **123**, 174701 (2005).